Grinding of calcite suspensions in a stirred media mill: Effect of operational parameters on the product quality and the specific energy

Soualo Ouattara, Christine Frances *

Université de Toulouse, INPT, UPS, LGC (Laboratoire de Génie Chimique), BP.84234, 4 Allée Emile Monso 31432 Toulouse Cedex 4, France
CNRS, LGC, F-31432 Toulouse Cedex 4, France

ARTICLE INFO

Keywords:
Wet grinding
Stirred media mill
Particle size
Rheology

ABSTRACT

This paper investigates the production of calcite suspensions by a wet grinding process in a stirred media mill. The experimental set-up allows the circulation mode process in the presence of sodium polyacrylate as additive. The influence of different operational parameters on grinding results in terms of particle size distribution and rheological behavior of the suspensions as well as the grinding efficiency is presented. We observe that the specific energy input that leads to a required product quality is not the same. Moreover, analyzing the trend of particle size versus the specific energy input instead of versus the grinding time, different and opposite conclusions flow from the experiment results. In addition, the effect of particle mean size on the suspension viscosity is presented.

1. Introduction

In the recent years, the industrial demand for ultrafine particles increased a lot due to the specific properties of nanoparticles, particularly in the chemical and pharmaceutical industries where products with high homogeneity or solubility are often required. Among product properties, particle fineness, expressed by the median size or the width of the particle size distribution is of prime importance. But other properties, as the suspension stability or rheological behavior are also important parameters for industrial applications. Stirred media milling has proven its ability to produce ultrafine particles in concentrated suspensions from a coarser product [1–3]. In such mills, the fragmentation results from the compression and shear induced by high speed rotating grinding beads with an agitator. It is known that a lot of parameters can affect the results of wet grinding and dispersion in stirred media mills. These parameters can be classified into four groups: grinding chamber and stirrer geometries, operating parameters (grinding time, stirrer tip speed, grinding bead filling ratio, bead size and properties, …), grinding operation mode (continuous, batch, pendular or circulating mode) and suspension formulation (solid concentration, particle size, additives, …). Many papers deal with the influence of different operating parameters on the grinding results. Research is usually conducted with two main objectives.

First, work aims to analyze the performance of the mill [4–8]. This approach is very interesting to get quantitative information on the energy required to grind a product and it gives a very good basis for mill design and extrapolation to an industrial scale. Indeed, the grinding process mainly depends on the specific energy input (SE) which is the total energy supplied to the grinding chamber related to the mass of the ground product. Since wet grinding processes are extremely energy intensive, the optimization of the process parameters is important to minimize the energy consumption. For a given particle suspension, the quality and the fineness of the product that can be obtained by a milling process are determined by the number of stress events undergone by the particles of the suspension, known as stress number (SN) and the stress intensity at each stress event, also known as stress intensity (SI). Thus, the optimization of the process parameters for a desired particle fineness, in particular the grinding media materials, the bead size and the stirrer tip speed, is usually done by evaluating the specific energy or the stress intensity [6–9]. Moreover, as pointed out by Kwade [5], the particles to be ground through a grinding process and the resulting fragments are not subjected to the same number of stresses neither to the same stress intensities. Thus the number of stress events SN and stress intensity SI can only be characterized by distributions, depending on the operating parameters. The width of the distribution of stress number is determined above all by the residence time distribution of the particles in the mill. While the width of the distribution of the stress intensity depends mainly on how the stress energies differ locally and over the grinding time. Recently, Yamamoto et al. [10,11] used DEM simulation to determine the velocity distributions of beads in a stirred mill and correlate the size reduction kinetics with the bead impact energy.

Second, other research is focused on ground product quality (fineness, suspension stability, surface properties, …) in relation with the end-use properties of the products. This second approach involves more products with high added value as cosmetics or drugs, usually produced in small quantities. It is also of prime importance for the production of nanoparticles. Indeed, in the sub-micron particle

* Corresponding author at: Université de Toulouse, INPT, UPS, LGC (Laboratoire de Génie Chimique), BP.84234, 4 Allée Emile Monso 31432 Toulouse Cedex 4, France. Tel.: +33 5 34 32 36 39; fax: +33 5 34 32 36 99.
E-mail address: Christine.Frances@ensiacet.fr (C. Frances).

https://doi.org/10.1016/j.powtec.2013.11.025

size range the behavior of the product suspensions is more and more influenced by increasing particle–particle interactions. Due to these interactions, agglomeration phenomena can occur limiting further size reduction and a fixed minimum particle size is reached whatever the operating conditions [12]. For the same reasons, the viscosity of the ground suspension often increases [13] and this affects the ability of the particles to be broken. Also, a lot of work focuses on the research of grinding additives [14–16] or operating conditions able to improve suspension stability during the grinding process [17]. In other recent papers, a bead milling process was even used to enhance dispersion stability [18] or to improve other end-use properties [19,20]. When the focus is on the properties of the ground product, the analysis of the grinding kinetics regarding the evolution of the particle size distribution or other desired properties versus the grinding time is of prime importance. Another important feature in stirred media milling is related to the bead wear and the possible contamination of the ground product [21,1], but this point is out of the scope of our paper.

In our work, we did not want to favor one or the other objective (energetic performance or product quality). Instead, we wanted to connect the two types of analysis to better understand the influence of some operating parameters and assist in their selection. Calcium carbonate was chosen as a model material since its behavior during stirred media milling is well representative of the majority of inorganic or organic materials. It is obvious that many parameters related to the mill geometry, the operating mode and to the formulation of the suspension, affect the grinding result. In this study, we investigated the influence on the grinding process of some of these different operating parameters and both interpreted the results in terms of grinding kinetics and specific energy. The rheological behavior of the suspension during the grinding process of particles is also studied for different operating conditions. Finally, the effect of particle mean size on suspension viscosity is highlighted.

2. Material and experimental device

A high pure (>99%) calcite ($CaCO_3$) obtained from Merck, Germany was used for the experiments. The density of this material is 2656 kg/m^3 at 20 °C and the median particle size at the initial state is about 30 μm (measured by laser diffraction). Moreover, sodium polyacrylate (SPA) from Sigma-Aldrich with a molecular weight of 5100 g/mol and a density of 550 kg/m^3 was used to disperse the particle of $CaCO_3$ in water. Garcia et al. [14] have shown that the use of this polyelectrolyte could help in processing calcite suspension avoiding the re-aggregation of fine fragments. The SPA concentration was kept constant at 8% (i.e. 8 g of SPA per 100 g of $CaCO_3$) for all the runs.

All the grinding experiments were performed in a laboratory stirred media mill (Labstar from Netzsch) using the circulation mode (Fig. 1). The initial suspension is put into a feed tank equipped with an agitator to ensure a good mixing preventing the formation of deposits or dead zones. During the run, the suspension is continuously pumped from the feed tank trough the stirred media mill by means of a peristaltic pump. The outlet of the mill is also connected to the feed tank allowing the ground product to go back into the feed tank. The power input delivered by the motor (M), the pressure (P) and the temperature (T) at the inlet and the outlet of the grinding chamber were continuously registered during the process.

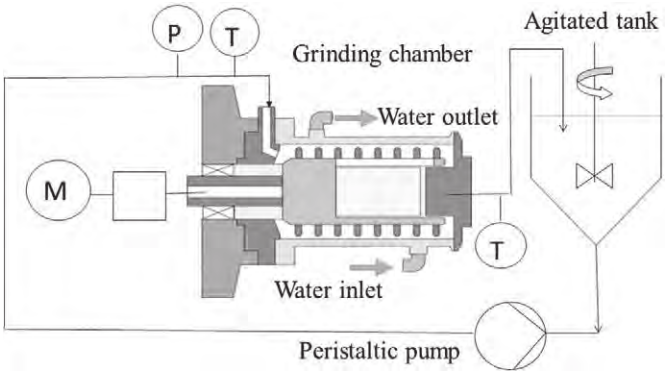

Fig. 1. Experimental set-up.

The determination of the specific energy depends among others on the mode of grinding operation. For a grinding process in a circulating mode (multi-passes), the specific energy can be determined as follows:

$$SE = \frac{\int_0^t (N(\tau) - N_0)\mathrm{d}\tau}{m_P} \quad (1)$$

Where m_P is the mass of the solid product, $N(\tau)$ is the power at the time τ and N_0 is the no-load power. If the grinding media wear is significant, especially, considering long grinding periods, a correction can be introduced [22] to take into account of it in the expression of the specific energy. In that case, it is assumed that the media wear increases proportionally to the power input N and the mass of the product is then extended by $0.5\Delta m_{GM}$, with Δm_{GM} the grinding media wear at the end time t of the grinding process. For our experimental study, the bead wear has been reduced, choosing high resistant beads (Y_2O_3-stabilized ZrO_2 media) and by using a grinding chamber and a separating cartridge lined with Cr–Ni-steel and equipping the agitator with tungsten–carbide. During the runs, the torque and the number of revolutions were automatically measured by a torque sensor put on the stirrer shaft, thus allowing calculating the specific energy using Eq. (1).

Moreover, samples were withdrawn over the run duration at the outlet of the grinding chamber. Particle size distribution was characterized by photon correlation spectroscopy (PCS) using a Nanosizer ZS (Malvern Instruments) in the nanometer size range. This apparatus gives access to the hydrodynamic diameter of the particles on the base of the Brownian diffusion.

Rheological measurements of the ground suspensions were also performed at ambient temperature using a rotational rheometer AR2000 (TA Instruments). A cone and plate geometry (60 mm diameter, 2° cone angle) was used. A pre-shearing step was imposed to ensure the same starting point for all the samples and then the shear rate was linearly decreased from 1000 to 0.1/s.

3. Effect of operational parameters

3.1. Effect of the volume flow rate

The effect of the volume flow rate on the grinding result is first discussed. Using the circulating mode, the residence time by pass and the number of passes are modified changing the flow rate. The residence time τ_p, of the suspension inside the grinding chamber by pass is equal to:

$$\tau_p = \frac{V_{GC} - V_{GB}}{Q_S} \quad (2)$$

where V_{GC} is the volume of the grinding chamber equipped with the agitator and the cartridge sieving, V_{GB} the true volume occupied by the beads (equal to the number of beads multiplied by the bead volume) and Q_s the suspension flow rate.

The suspension volume V_s and the full operation time t being fixed, an increase of the flow rate implies a decrease of the suspension residence time by pass, but also an increase of the number of passes during the full operation time. Thus, the true residence time of the suspension during a grinding run in the circulation mode is given by:

$$\tau_s = t\frac{(V_{GC} - V_{GB})}{V_s}. \quad (3)$$

Table 1
Residence time by pass and number of passes for different volume flow rates.

	Rotation speed of the pump (rpm)			
	50	70	90	120
Volume flow rate (10^{-6} m^3/s)	5.0	7.2	8.8	11.7
Residence time by pass (s)	51	35	29	22
Number of passes for t = 10 min	12	17	21	28
Number of passes for t = 30 min	35	51	62	83
Number of passes for t = 1 h	71	103	124	166
Number of passes for t = 6 h	423	615	743	995

So over a given run time, the mean residence time of the suspension in the grinding zone is the same whatever the flow rate and no effect of the flow rate on the grinding result is expected. However, the flow rate could have an effect on the hydrodynamics within the grinding chamber and affect indirectly the grinding result.

Several runs were performed using different flow rates *Qs* from 5×10^{-6} m^3/s (18.0 l/h) to 11.75×10^{-6} m^3/s (42.3 l/h). For these runs, the stirrer tip speed was kept constant at 5.7 m/s (equivalent to a rotational speed of 1500 rpm). Details on the experimental conditions, number of passes and suspension residence times are reported in Table 1. These runs were done using Y_2O_3-stabilized ZrO_2 grinding media (the bead diameter is between 300 and 500 μm and the bead density is 3785 kg/m^3). The bead filling volume was kept constant at 75% and the solid mass fraction c_m at 0.2. The evolution of the particle mean size (hydrodynamic mean diameter, also called Z-average) versus the grinding time are reported in Fig. 2.

It can be seen that the flow rate has a slight effect on the particle size during the first thirty minutes of the process. Several passes are thus necessary to counteract the volume flow rate effect. After that, no significant difference on the particle size distribution was observed. This result is consistent with conclusions given by Gers et al. [23] based on direct numerical simulation of the hydrodynamics of a stirred media mill. It was shown that the flow rate in the grinding chamber (between 0 and 100 l/h) did not modify or had no effect on the hydrodynamic conditions since the effect generated by the axial flow of the material was insignificant compared to the strains resulting from the rotation of the agitator. Thus the volume flow rate of the suspension is a parameter of minor importance, but it is important to keep in mind that the particle size distribution of ground samples taken during the first minutes of the process can slightly be influenced by the suspension flow rate. This parameter was then kept constant for all the experiments described below.

3.2. Effect of the stirrer tip speed

Contrarily to the flow rate, it is obvious that the stirrer speed is an important operating parameter insofar as it affects simultaneously the number of collisions between beads and the intensity of these collisions.

To investigate the influence of the stirrer speed on the grinding results, experiments with different stirrer tip speeds (5.7, 7.7, and 9.6 m/s) were performed. These tip speeds correspond respectively to rotational speeds of 1500, 2000 and 2500 rpm. The other conditions were identical to those mentioned above. The evolution of the median size of particles is plotted as function of the grinding time in Fig. 3a. Whatever the stirred speed, the median size decreases versus time, rapidly during the first period and then more slowly. Increasing the stirrer speed, the grinding process is faster and a finer product is obtained for a fixed grinding time. These results are in accordance with those of Hennart et al. [12] concerning the size reduction of a poorly soluble organic compound in a stirred media mill.

Since the stirrer speed affects the collision intensity between beads, and hence the specific energy, it can be also interesting to analyze the effect of this parameter as function of the specific energy input. The specific energy input is the ratio of the total energy supplied to the grinding chamber to the product mass. The effect of stirrer tip speed on specific energy input is illustrated in the Fig. 3b. Increasing the stirrer speed and hence the specific energy input, the initial size reduction of particles is increased. For specific energies less than 5×10^3 kJ/kg the results show identical particle size whatever the stirrer tip speed applied. For specific energies between 5×10^3 kJ/kg and 2×10^4 kJ/kg, the influence of stirrer speed is insignificant but finer particles are obtained with the lowest stirrer speed. Under these conditions, in terms of energy efficiency, the best result is obtained with a stirrer speed of 5.7 m/s (1500 rpm). However, up to a specific energy of 2×10^4 kJ/kg, the stress energy is not sufficient to produce ultra-fine particles (<100 nm). Thus, more stress events, i.e. a higher energy input, are necessary. Fine particles are thus obtained with the higher stirrer speed (9.6 m/s or 2500 rpm). It would take a much longer process time with lowest stirrer speeds to eventually reach such fineness.

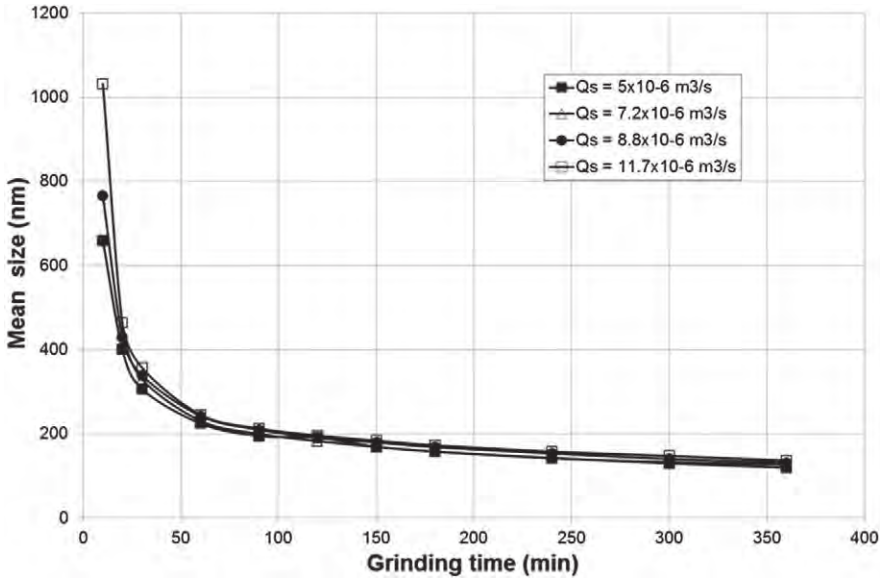

Fig. 2. Effect of the volume flow rate on the grinding result.

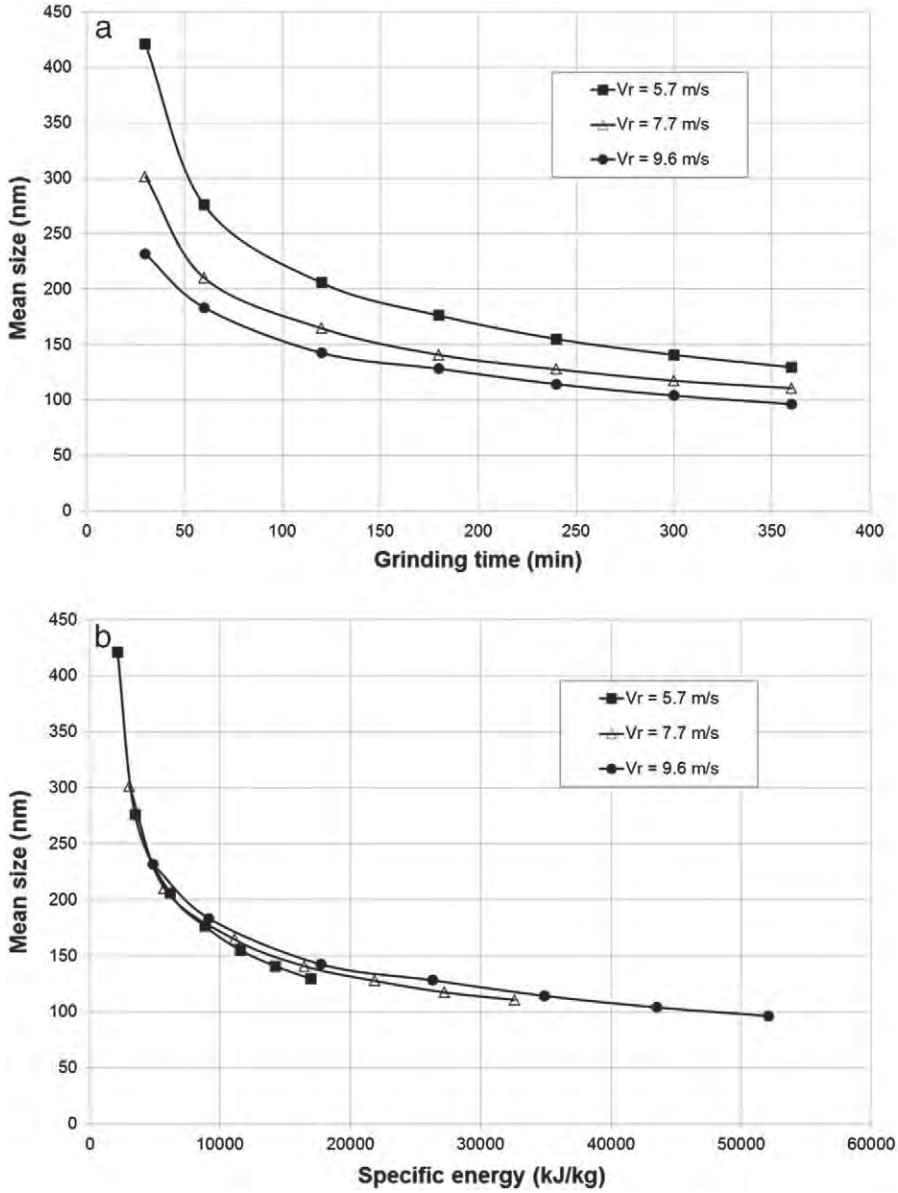

Fig. 3. Effect of stirrer tip speed on grinding result. a) Particle mean size versus grinding time. b) Particle mean size versus specific energy.

Moreover, considering now the whole size distribution and not only the mean size, it can be observed in Fig. 4a, corresponding to a specific energy close to 1.7×10^4 kJ/kg that the particle size distributions are nearly similar imposing different stirrer tip speeds. The size distribution ranges between 20 and 600 nm for the three considered speeds. We can notice that the particle size distributions are bimodal revealing the presence of a small amount of very small fragments (around 30 nm) more particularly applying a high stirrer tip speed, whereas this population is less noticeable for the lowest tip speed. Globally, the stirrer tip speed has little influence on the fragment size distribution when rather low and equivalent specific energies are considered. Instead, its influence is evident for identical grinding process times. To illustrate this purpose, the particle size distribution of ground suspensions recovered after 6 h for each run are reported in Fig. 4b.

3.3. Effect of the solid mass concentration

In order to investigate the influence of the solid mass concentration, different calcite suspensions were prepared reducing the solid mass fraction from 0.3 to 0.05. For all the experiments, the stirrer speed was fixed at 5.7 m/s (1500 rpm) and grinding beads of 300 to 500 μm in diameter were used. The bead filling volume inside the grinding chamber was kept constant at 75%. We can observe in Fig. 5a, that whatever the chosen time, finer particles are obtained decreasing the solid concentration. This result agrees well with the observations of Choi et al. [24] who showed that the lower the calcite solid concentration, the better was the grinding rate. Analyzing again the results in term of specific energy (see Fig. 5b), other conclusions can be drawn. Indeed, finer particles were obtained for higher solid mass fractions at identical energy inputs. Thus, less than 10^4 kJ/kg is necessary to produce median particle size of around 180 nm with a mass fraction $c_m = 0.2$, whereas with a mass fraction $c_m = 0.05$ the same median particle size is obtained with a specific energy three times higher (3×10^4 kJ/kg). This result is coherent with the one observed by Stenger et al. [25] in the case of alumina.

Again, it can be interesting to analyze the full PSD. The PSD of ground suspension at different solid mass concentrations for a specific energy of about 1×10^4 KJ/kg has been reported in Fig. 6. For this given specific

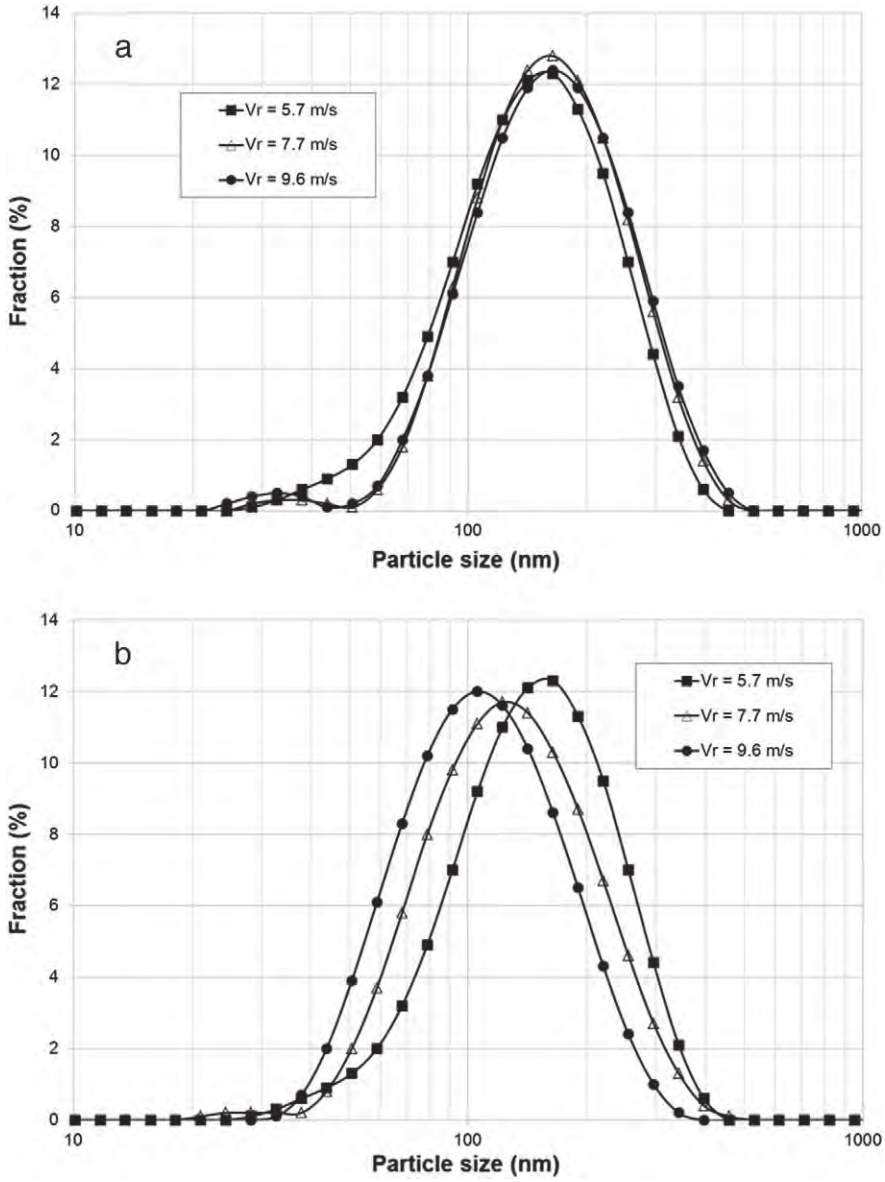

Fig. 4. Effect of stirrer tip speed on grinding result. a) PSD of ground suspensions for $E_s = 1.74 \times 10^4$ kJ/kg. b) PSD of ground suspensions recovered after 6 h of the process.

energy, the size distribution is bimodal showing a small amount of fine fragments around 40 nm for the highest concentrated suspensions. The distributions spread between 30 and 700 nm for the solid concentrations of 0.1, 0.2 and 0.3. The best fineness seems to be reach for the intermediate solid concentration equal to 0.2. This result will be commented in Section 4. For the lowest concentration ($c_m = 0.05$), coarse particles, until 1500 nm, are present. The specific energy being inversely proportional to the solid concentration, it must be noticed that at this low concentration, the grinding time corresponding to the chosen specific energy is around 1 h. In these conditions and due to the low mass concentration, the probability that all particles will be captured and stressed enough to be broken is low. As a result, a larger PSD is obtained.

4. Rheological behavior of the ground suspension

During a grinding process, due to decreasing product particle sizes, particle–particle interactions increase. So the viscosity of the ground suspensions often increases during batch processes and problems can arise with the separation system (cartridge in our case) which enables the suspension to get out of the grinding chamber keeping the beads inside. The rheological properties are also an important criterion for product quality in many industrial applications.

The evolution of the viscosity as function of the grinding time was determined for runs performed with different solid mass concentrations ($c_m = 0.1$, $c_m = 0.2$ and $c_m = 0.3$). As an example, the viscosity versus the shear rate is plotted in Fig. 7 for the run performed with the solid mass concentration of 0.3 and a stirrer tip speed of 5.7 m/s (1500 rpm). It can be seen that the ground suspensions have a shear thinning behavior. For the lower concentrated ground suspensions, it was observed that they behave as Newtonian fluids.

Furthermore we observed that the higher was the solid mass fraction, the higher was the viscosity of the suspension. As a matter of fact, according to Ding et al. [26], for low solid mass fractions, the inter-particle distance is large enough to keep away the particles from each other and the particles can move in a free individual motion. That enhances in addition, suspension fluidity. A high solid mass fraction induces a short mean inter-particle distance, and the particle–particle interactions become

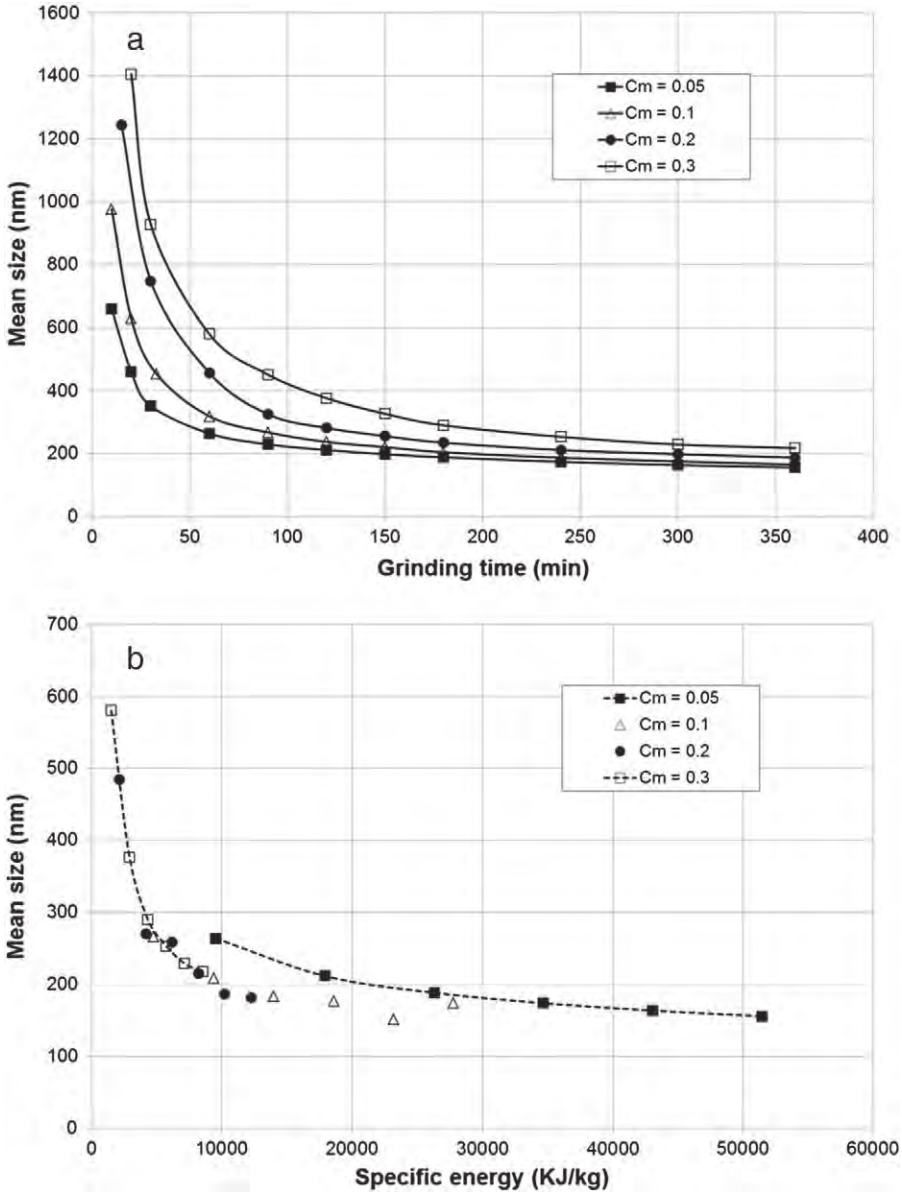

Fig. 5. Effect of solid mass concentration on the grinding result. a) Particle mean size versus grinding time. b) Particle mean size versus specific energy.

more prevalent. So the free motion of particles is disturbed [27]. Partial aggregation phenomena can also occur, leading to an important rheological change as it can be seen for mass fraction of 0.3 in Fig. 7. So, increasing the solid concentration, the suspension fluidity decreases and this can explain why a poorer fineness was obtained for a solid concentration of $c_m = 0.3$ than for a lower solid concentration.

To highlight the effect of the presence of a dispersed phase in a suspension, different authors investigated the relation between the suspension viscosity, the continuous phase viscosity, and the particle volume fraction. For low particle volume fractions, the viscosity is generally independent of the shear rate and can be connected to the volume fraction by Epstein's equation [28]:

$$\eta_{susp} = \eta_0\left(1+\frac{5}{2}c_v\right). \tag{4}$$

In Fig. 8, ratio of the suspension viscosity (for a shear rate of 200 s^{-1}) to liquid viscosity is presented as a function of the volume fraction for different suspensions of ground calcite. The curve corresponding to Epstein equation is also reported in this figure. We can observe that Eq. (4) valid for hard spheres in diluted conditions (usually $c_v \leq 0.07$), underestimates the viscosities. This result is not surprising, due to the fact that calcite particles are not mono-disperse, neither spherical, and that the considered suspensions are more concentrated than the ideal case predicted. For concentrated suspensions, several relationships were established. Among them is Krieger–Dougherty relationship [29]:

$$\eta_{susp} = \eta_0\left[1-\frac{c_v}{c_{\max}}\right]^{-[\eta]c_{\max}} \tag{5}$$

where c_{max} is the maximum fraction of stacking. It depends on the size distribution of particles, on their shape and their arrangement ($c_{max} \approx 0.55$ for dispersed random stacking and $c_{max} \approx 0.65$ for dense random stacking).

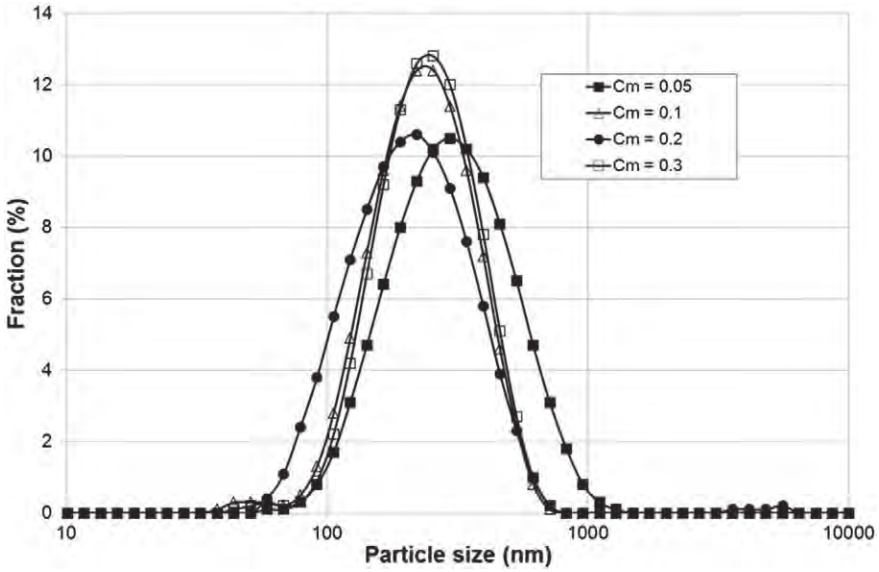

Fig. 6. Effect of the solid mass concentration on the PSD for a specific energy of 1×10^4 kJ/kg.

Krieger–Dougherty's equation can be re-written as follows:

$$\ln\left(\frac{\eta_{susp}}{\eta_0}\right) = -[\eta]c_{\max}\ln\left(1-\frac{c_v}{c_{\max}}\right). \quad (6)$$

Assuming that $c_{max} = 0.63$ and plotting the characteristic line of Eq. (6), we obtained a value of $-[\eta]c_{max}$ equal to − 6.7 ($[\eta] = 10.6$).

In the case of hard spheres, the intrinsic viscosity $[\eta]$ equals to 2.5. The intrinsic viscosity value obtained in our study is then higher and that can be explained by the fact that the particles of the suspensions are not spherical, polydispersed and are likely to develop interparticle interactions. Furthermore c_{max} and $[\eta]$ depend on the applied shear rate.

The viscosities calculated by the Krieger–Dougherty equation taking into account the value of 10.6 for the intrinsic viscosity is also reported in Fig. 8. The experimental points are close to the Krieger–Dougherty correlation. It is then obvious that this correlation can be used to model the viscosity of ground calcite suspensions.

To investigate the influence of the stirrer tip speed used during the grinding process on the rheological behavior of the ground suspensions, samples were withdrawn during the runs from time to time over the whole period of 6 h and analyzed using the same rheological procedure as described before. For the lowest stirrer tip speed used (5.7 m/s or 1500 rpm), practically no change on the suspension's viscosity was observed during the grinding time. The suspension had a quasi-Newtonian behavior. However, for experiments carried out at higher stirrer tip speeds (7.7 and 9.6 m/s, corresponding respectively to the rotational speeds of 2000 and 2500 rpm), the suspensions presented a shear thinning behavior (i.e. the viscosity decreases with increasing shear rate). An example is reported in Fig. 9. corresponding to the run performed with the tip speed 9.6 m/s (2500 rpm) and a solid concentration $c_m = 0.2$. The thinning behavior is clearly shown in Fig. 9 for the suspensions obtained after 3 h to 6 h. For shorter grinding periods, the suspensions behave as Newtonian fluids. The increase observed versus the shear rate for the two curves corresponding to $t = 1$ h and $t = 2$ h results from inertia effects using the cone and plate geometry

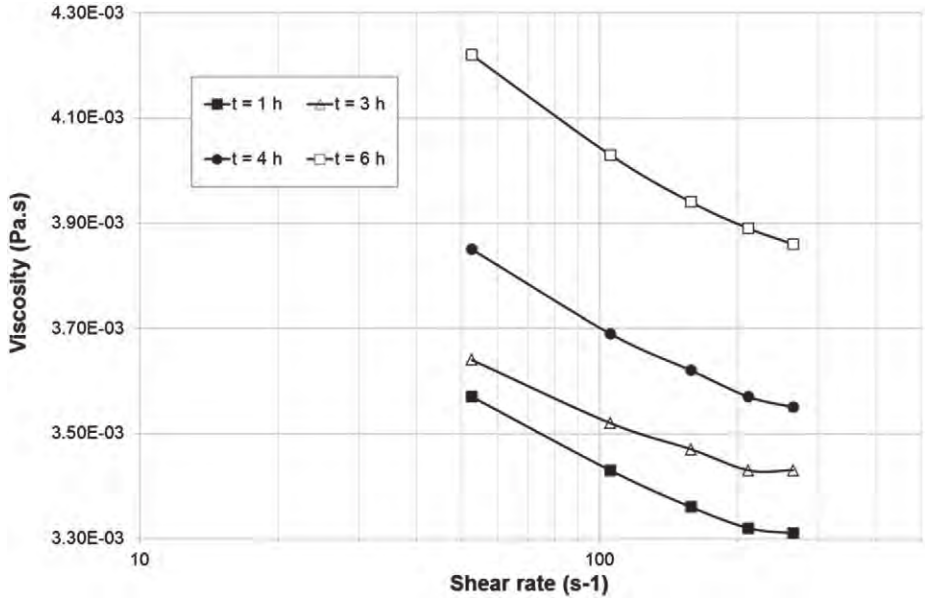

Fig. 7. Evolution of suspension viscosity ($V_r = 5.7$ m/s, $c_m = 0.3$) as function of shear rate for different grinding times.

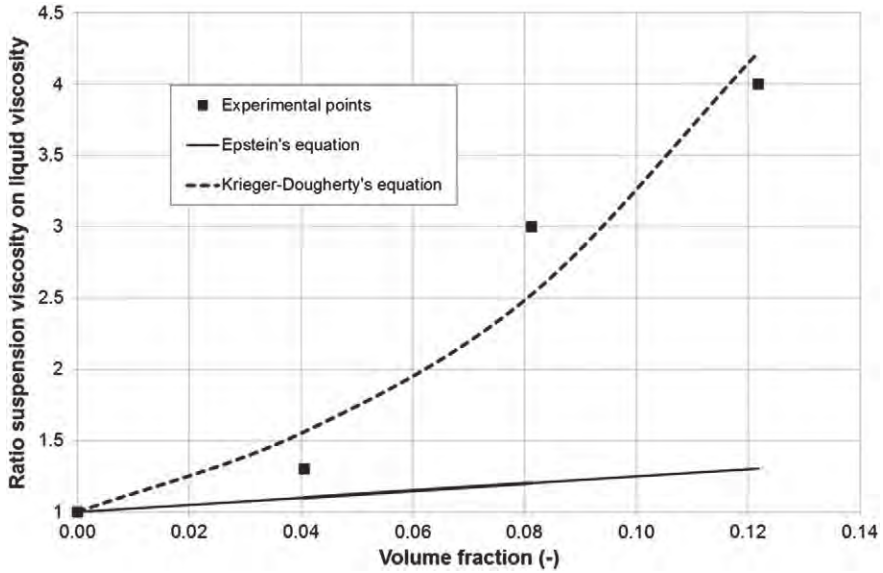

Fig. 8. Ratio of the suspension viscosity (η_{susp}) to liquid viscosity (η_0) as function of the volume fraction for different suspensions of ground calcite.

for such poorly viscous fluids. Moreover, whatever the stirrer speed at which the run was performed, the viscosity increases for a given shear rate as the time needed to ground the suspension in the mill increases.

And finally, the higher was the stirrer tip speed during the grinding process, the more viscous were the suspensions. Increasing the stirrer tip speed promotes the production of finer particles. Thus, we investigated the effect of the particle size on the suspension viscosity. We observe a clear dependence of the viscosity with the particle median size (Fig. 10). When the mean particle sizes are above 150 nm, the suspension viscosity is low and constant whatever the particle size. In the contrary, when the suspension contains particles of a mean size below 150 nm, the viscosity increases exponentially. This can be explained by the fact that for a given solid concentration, when the particle size decreases, the interparticle distance in the suspension also decreases. Hence, the particles cannot move any more freely from each other, leading to an increase of the suspension viscosity. Concerning calcite grinding, the trend reported on the evolution of the apparent viscosity versus the mean particle size explains why it is difficult to reach fineness less than about 150 nm, even using a dispersing agent and with moderate solid concentrations. So, the suspension viscosity is a key factor to control the size reduction process in the sub-micronic range.

5. Conclusions

The effect of some operational parameters on the wet grinding of calcite suspension was investigated. The results are discussed on the base of the product quality (particle fineness and rheological behavior of the ground suspension) as well as energy efficiency. Increasing the stirred speed or decreasing the solid mass concentration, the time necessary to get ultrafine particles decreases. However for a given product particle size (150 or 200 nm for example), a lower specific energy is needed using a low stirrer speed or a rather high solid mass concentration. Moreover, it was shown that the suspension viscosity can be well described as function of the solid volume fraction by the Krieger–Dougherty's equation. For a given volume fraction, a correlation was also observed between the apparent viscosity and particle fineness whatever the operational conditions applied.

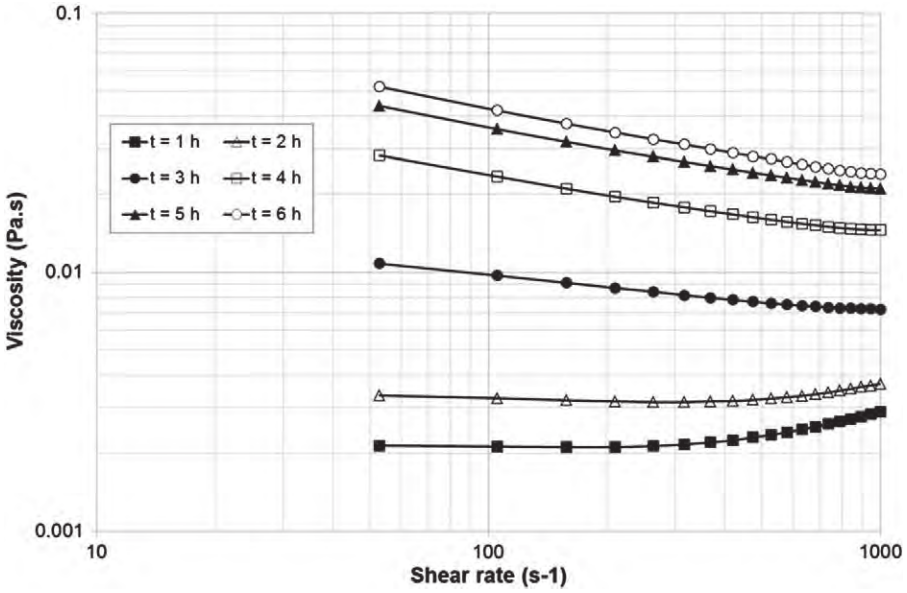

Fig. 9. Evolution of suspension viscosity ($V_r = 9.6$ m/s, $c_m = 0.2$) versus the shear rate for different grinding times.

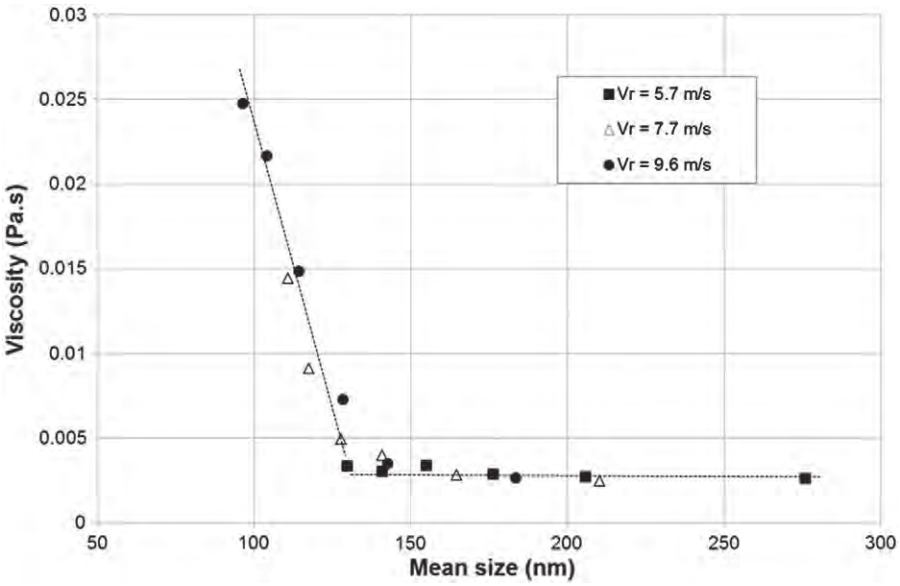

Fig. 10. Evolution of suspension viscosity as function of median size of ground calcite for various stirrer speeds imposed during the grinding process.

References

[1] S. Mende, F. Stenger, W. Peukert, J. Schwedes, Mechanical production and stabilization of submicron particles in stirred media mills, Powder Technol. 132 (2003) 64–73.

[2] F. Stenger, S. Mende, J. Schwedes, W. Peukert, The influence of suspensions properties on the grinding behaviour of alumina particles in the sub-micron size range in stirred media mills, Powder Technol. 156 (2-3) (2005) 103–110.

[3] F. Stenger, M. Götzinger, P. Jakob, W. Peukert, Mechanochemical changes of nanosized α-Al_2O_3 during wet dispersing in stirred ball mills, Part. Part. Syst. Charact. 21 (1) (2004) 31–38.

[4] A. Kwade, J. Schwedes, Breaking characteristics of different materials and their effects on stress intensity and stress number in stirred media mills, Powder Technol. 122 (2002) 109–121.

[5] A. Kwade, Mill selection and process optimization using a physical grinding model, Int. J. Miner. Process. 74S (2004) S93–S101.

[6] U. Weber, The effect of grinding media performance on milling a water-based color pigment, Chem. Eng. Technol. 33 (9) (2010) 1456–1463.

[7] U. Weber, D. Langlois, The effect of grinding media performance on milling and operational behaviour, J. South. Afr. Inst. Min. Metall. 110 (3) (2010) 147–152.

[8] S. Breitung-Faes, A. Kwade, Prediction of energy effective grinding conditions, Miner. Eng. 43–44 (2013) 36–43.

[9] S.L.A. Hennart, P. van Hee, V. Drouet, M.C. Domingues, W.J. Wildeboer, G.M.H. Meesters, Characterization and modelling of a sub-micron milling process limited by agglomeration, Chem. Eng. Sci. 71 (2012) 484–495.

[10] Y. Yamamoto, R. Soda, J. Kano, F. Saito, DEM simulation of bead motion during wet bead milling using an enlarged particle model, Int. J. Miner. Process. 114–117 (2012) 93–99.

[11] Y. Yamamoto, R. Soda, J. Kano, F. Saito, Dispersion of carbon black by a media mill and correlation of its rate constant with beads, Powder Technol. 219 (2012) 105–110.

[12] S.L.A. Hennart, M.C. Domingues, W.J. Wildeboer, P. van Hee, G.M.H. Meesters, Study of the process of stirred ball milling of poorly water soluble organic products using factorial design, Powder Technol. 198 (1) (2010) 56–60.

[13] F. Garcia, N. Le Bolay, C. Frances, Changes of surface and volume properties of calcite during batch wet grinding process, Chem. Eng. J. 85 (2–3) (2002) 177–187.

[14] F. Garcia, N. Le Bolay, J. Trompette, C. Frances, On the fragmentation and agglomeration phenomena in an ultrafine wet grinding process: the role of polyelectrolyte additives, Int. J. Miner. Process. 74S (2004) S43–S54.

[15] H. Choi, W. Lee, S. Kim, Effect of grinding aids on the kinetics of fine grinding energy consumed of calcite powders by a stirred ball mill, Adv. Powder Technol. 20 (4) (2009) 350–354.

[16] H. Choi, W. Lee, D.U. Kim, S. Kumar, S.S. Kim, H.S. Chung, J.H. Kim, Y.C. Ahn, Effect of grinding aids on the grinding energy consumed during grinding of calcite in a stirred ball mill, Miner. Eng. 23 (1) (2010) 54–57.

[17] S.L.A. Hennart, W.J. Wildeboer, P. van Hee, G.M.H. Meesters, Stability of particle suspensions after fine grinding, Powder Technol. 199 (3) (2010) 226–231.

[18] I.M. Joni, A. Purwanto, F. Iskandar, K. Okuyama, Dispersion stability enhancement of titania nanoparticles in organic solvent using a bead mill process, Ind. Eng. Chem. Res. 48 (15) (2009) 6916–6922.

[19] M. Takeda, E. Tanabe, T. Iwaki, A. Yabuki, K. Okuyama, Preparation of nanocomposite microspheres containing high concentration of TiO_2 nanoparticles via bead mill dispersion in organic solvent, Chem. Lett. 38 (5) (2009) 448–449.

[20] I.M. Joni, T. Nishiwaki, K. Okuyama, S. Isoi, R. Kuribayashi, Enhancement of the thermal stability and mechanical properties of a PMMA/aluminium trihydroxide composite synthesized via bead milling, Powder Technol. 204 (1) (2010) 145–153.

[21] M. Becker, J. Schwedes, Comminution of ceramics in stirred media mills and wear of grinding beads, Powder Technol. 105 (1999) 374–381.

[22] A. Kwade, J. Schwedes, Wet grinding in stirred media mills, Handb. Powder Technol. (2007) 251–382(Chapter 6).

[23] R. Gers, E. Climent, D. legendre, D. Anne-Archard, C. Frances, Numerical modelling of grinding in a stirred media mill: hydrodynamics and collision characteristics, Chem. Eng. Sci. 65 (2010) 2052–2064.

[24] H. Choi, W. Lee, S. Kim, H. Chung, Effect of the sample concentration on the submicrometer particles produced during a stirred ball milling of calcite powders, Int. J. Appl. Ceram. Technol. 8 (5) (2011) 1147–1152.

[25] F. Stenger, W. Peukert, S. Mende, J. Schwedes, Nanomilling in stirred media mill, Chem. Eng. Sci. 60 (2005) 4557–4565.

[26] Z. Ding, Z. Yin, L. Liu, Q. Chen, Effect of grinding parameters on the rheology of pyrite–heptane slurry in a laboratory stirred media mill, Miner. Eng. 20 (2007) 701–709.

[27] M. He, Y. Wang, E. Forssberg, Parameter effects on wet ultrafine grinding of limestone through slurry rheology in stirred media mill, Powder Technol. 161 (2006) 10–21.

[28] P.S. Epstein, R.R. Carhart, The absorption of sound suspensions and emulsions. I. Water fog in air, J. Acoust. Soc. Am. 25 (1953) 533–565.

[29] I.M. Krieger, T.J. Dougherty, Trans. Soc. Rheol. 3 (1959) 137.